Better cloud calibration leads to improved realism in global atmospheric simulation

Po-Lun Ma

March 9, 2020

Biases in EAMv1

SWCRE

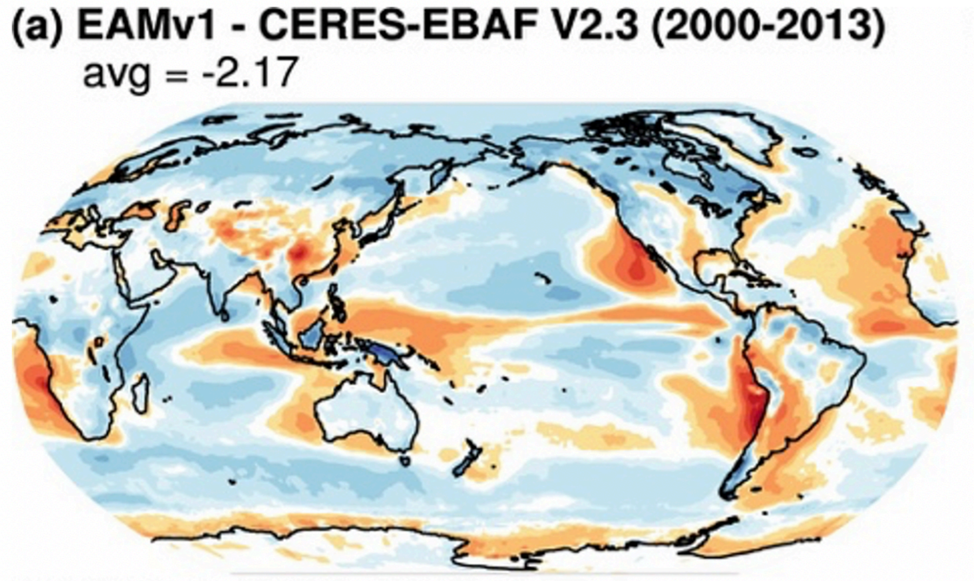

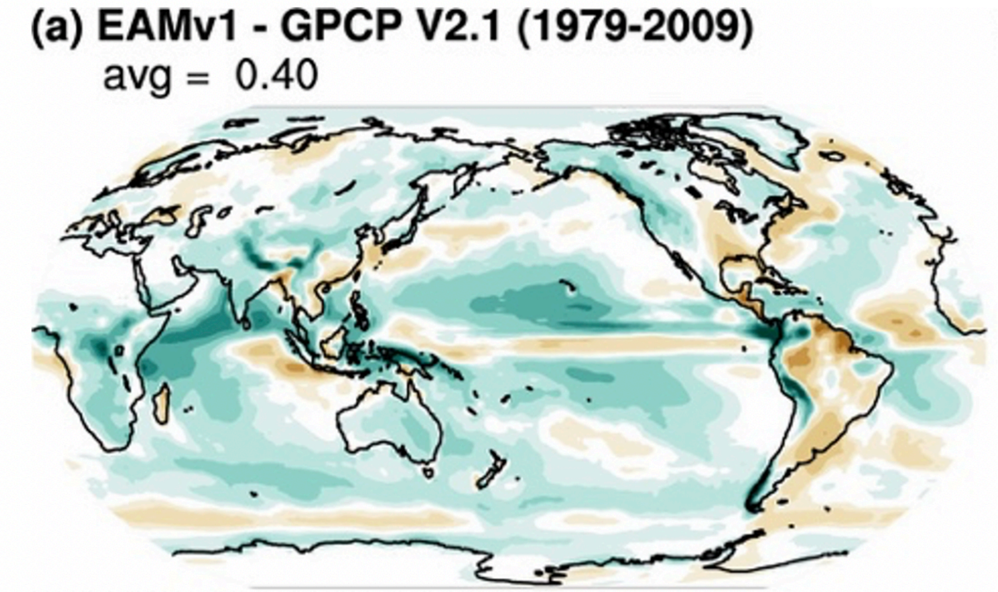

Precipitation

Surface winds

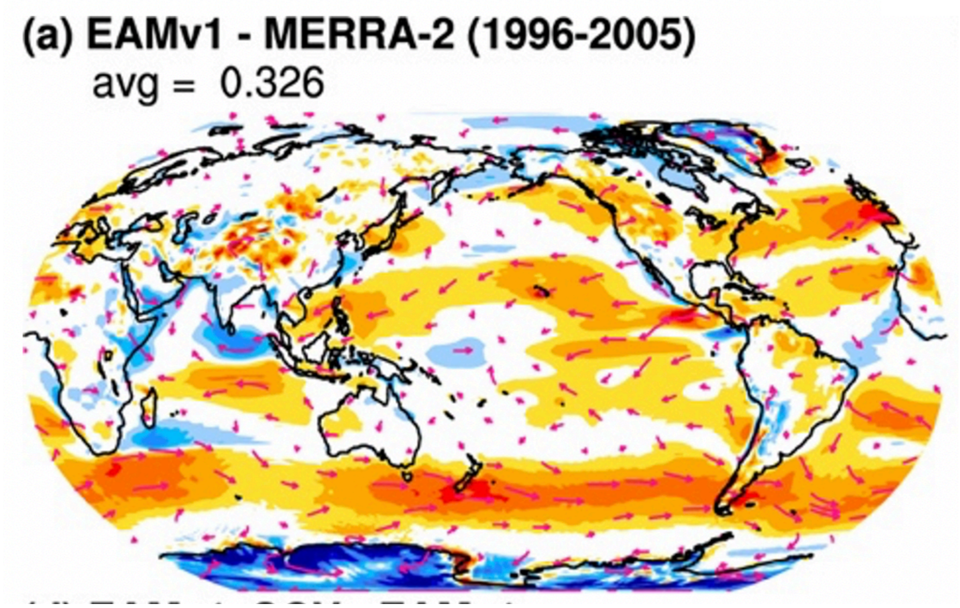

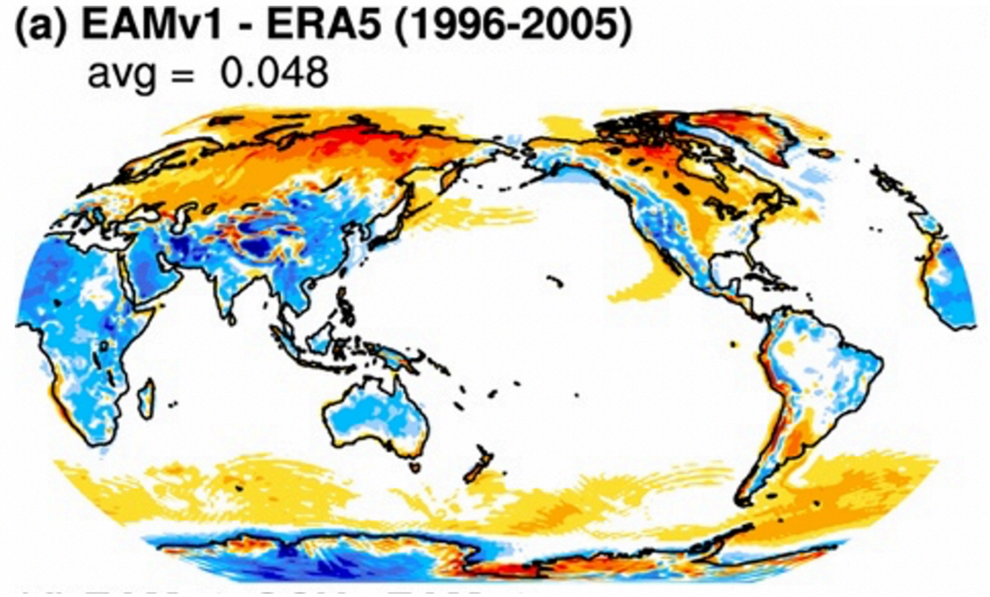

Surface temperature

PBL diagnostics provides insights into low cloud bias

EIS

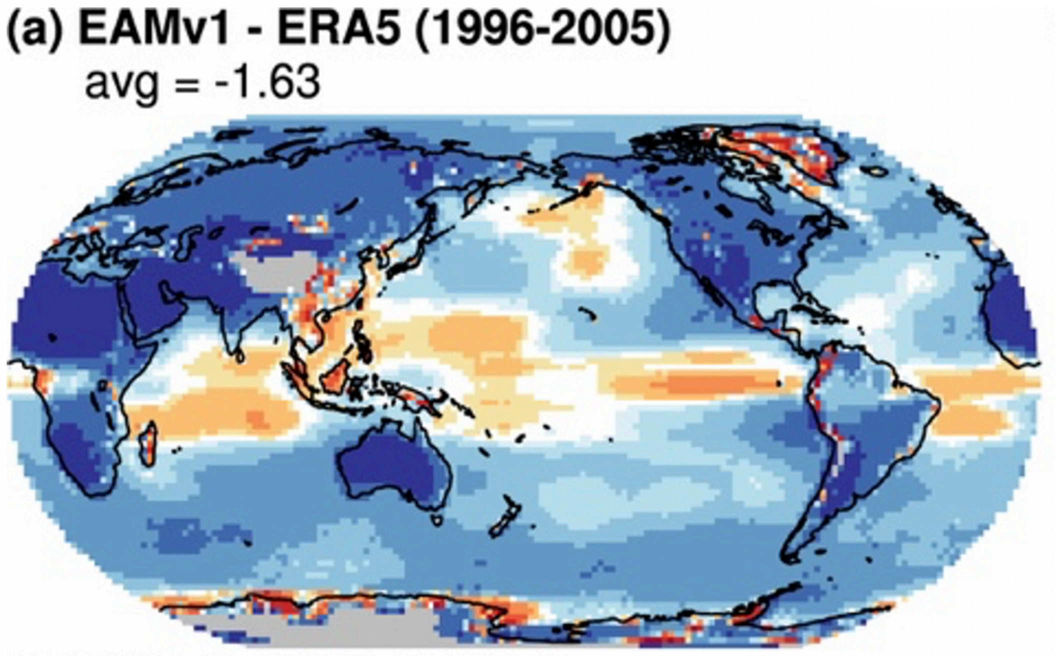

Decoupling frequency

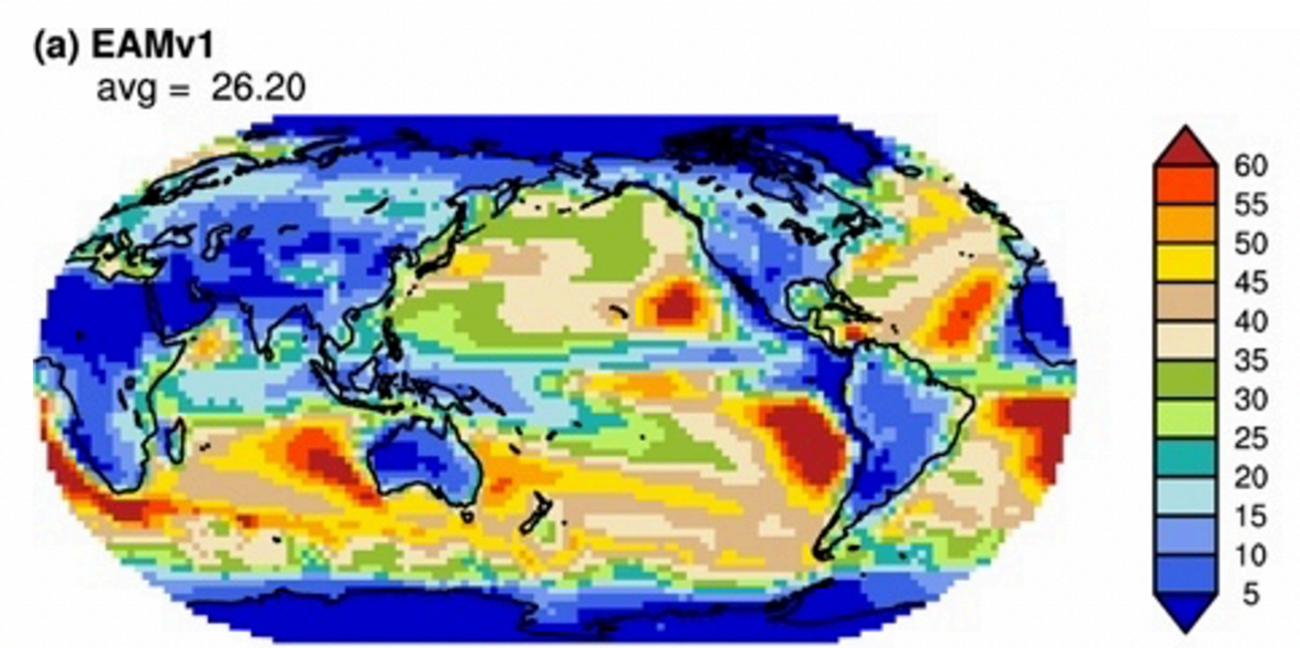

Neglecting subgrid winds might contribute to precipitation bias

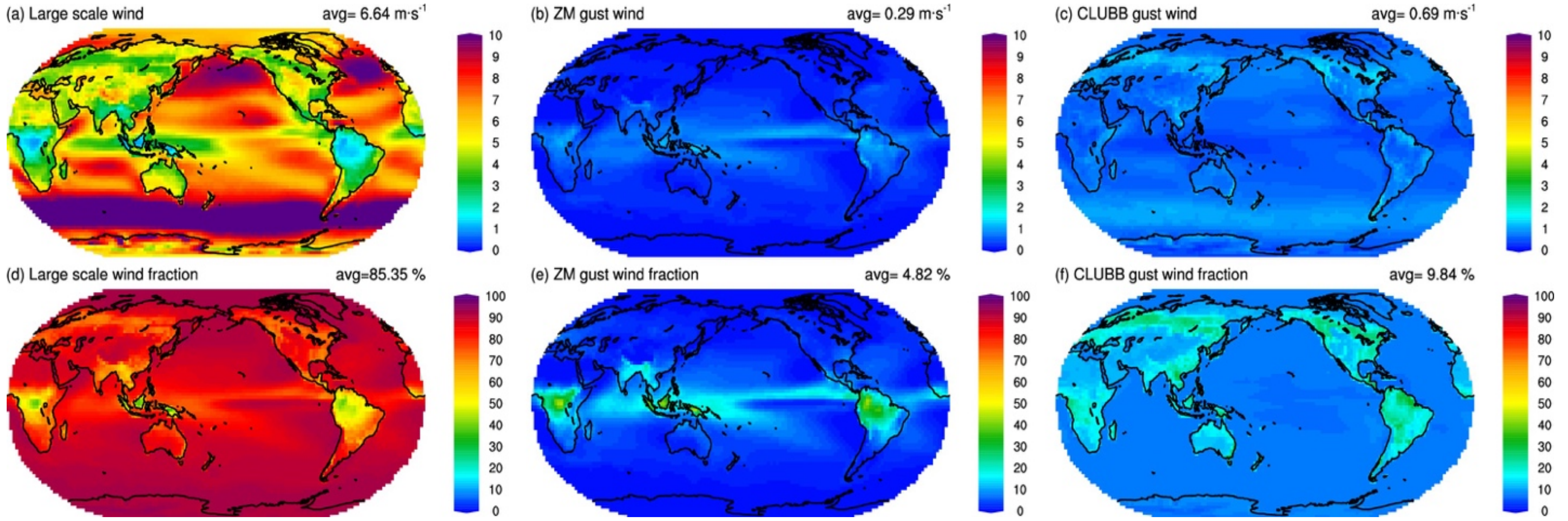

EAMv1 vs. subsequent changes

- **EAMv1**: Standard EAMv1 model
- **EAMv1_CLUBB**: EAMv1 + CLUBB tunings + skewness
- **EAMv1_SGV**: EAMv1+ ZM and CLUBB gustiness over land and ocean, subgrid temperature
- **EAMv1_MP**: EAMv1 + MG2 tunings
- **EAMv1_ZM**: EAMv1 + ZM tunings
- **EAMv1P**: EAMv1 + all changes

Skewness

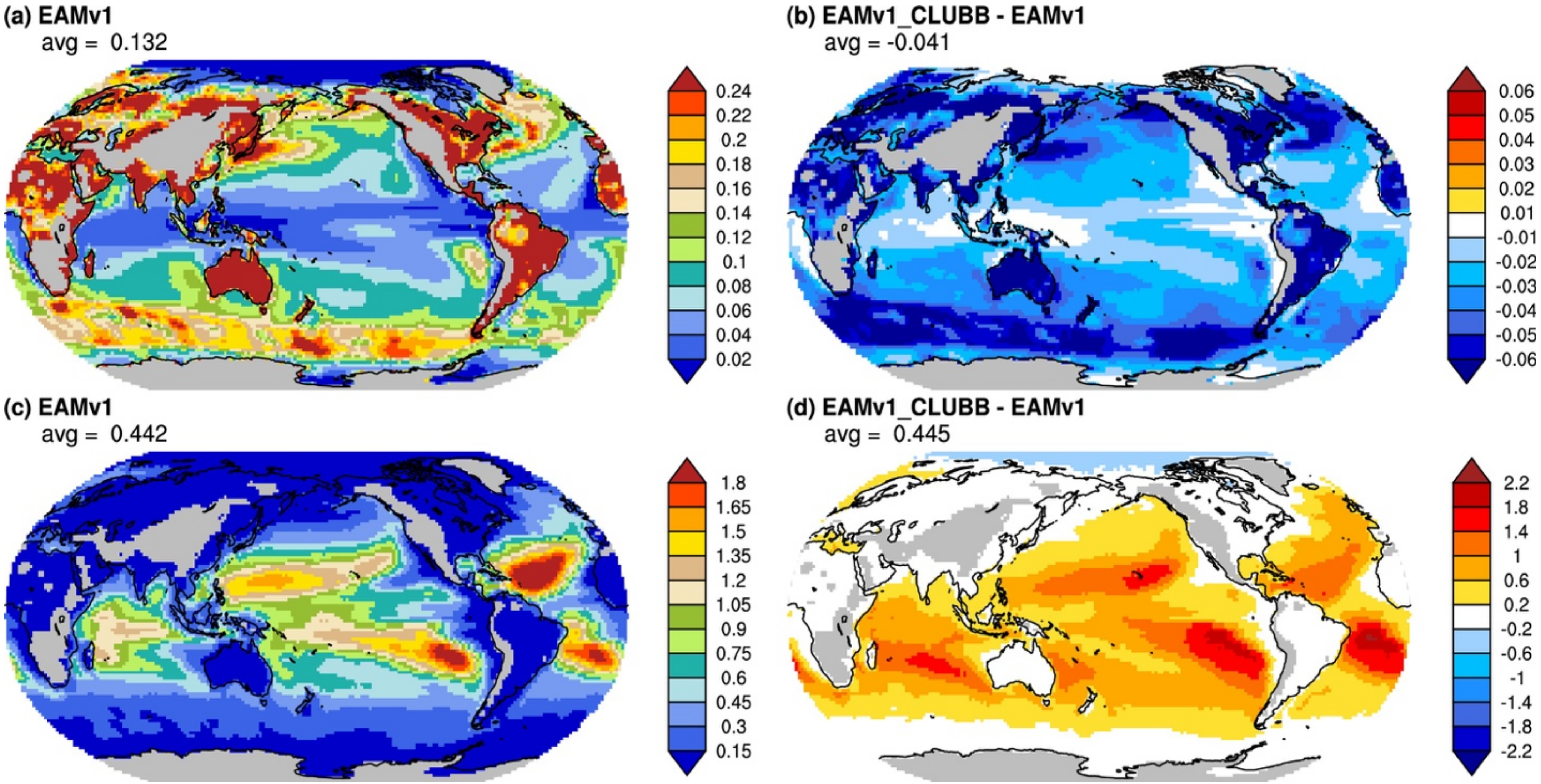
(a) EAMv1
avg = 0.132
0.24
0.22
0.2
0.18
0.16
0.14
0.12
0.1
0.08
0.06
0.04
0.02
(b) EAMv1_CLUBB - EAMv1
avg = -0.041
0.06
0.05
0.04
0.03
0.02
0.01
-0.01
-0.02
-0.03
-0.04
-0.05
-0.06
(c) EAMv1
avg = 0.442
1.8
1.65
1.5
1.35
1.2
1.05
0.9
0.75
0.6
0.45
0.3
0.15
(d) EAMv1_CLUBB - EAMv1
avg = 0.445
2.2
1.8
1.4
1
0.6
0.2
-0.2
-0.6
-1
-1.4
-1.8
-2.2

CLUBB Changes	Description	EAMv1	EAMv1P
C1	Coefficient for $\overline{w'^2}$ damping at low Sk_w	1.335	2.4
C1b	Coefficient for $\overline{w'^2}$ damping at high Sk_w	1.335	2.8
C1c	Coefficient for Sk_w dependency of C1*	1.0	0.75
C6rtb	Coefficient for $\overline{w'q_t'}$ damping at high Sk_w	6.0	7.5
C6rtc	Coefficient for Sk_w dependency of C6rt*	1.0	0.5
C6rthlb	Coefficient for $\overline{w'\theta_l'}$ damping at high Sk_w	6.0	7.5
C6rthlc	Coefficient for Sk_w dependency of C6rthl*	1.0	0.5
C8	Coefficient for $\overline{w'^3}$ damping	4.3	5.2
C11	Coefficient for $\overline{w'^3}$ damping at low Sk_w	0.80	0.7
C11b	Coefficient for $\overline{w'^3}$ damping at high Sk_w	0.35	0.2
C11c	Coefficient for Sk_w dependency of C11*	0.5	0.85
C14	Coefficient for $\overline{u'^2}$ and $\overline{v'^2}$ damping	1.06	2.0
C_k10	Ratio of eddy diffusivity of momentum to heat	0.30	0.35
gamma_coef	The width of the Gaussian PDF at low Sk_w	0.32	0.12
gamma_coefb	The width of the Gaussian PDF at high Sk_w	0.32	0.28
gamma_coefc	Coefficient for Sk_w dependency of the Gaussain PDF width	5.0	1.2
mu	Fractional entrainment rate	1.e-3	5.e-4
wpxp_l_thresh	Eddy length scale threshold for damping C6 and C7	60	100

MG2 Changes	Description	EAMv1	EAMv1P
cld_sed	Liquid droplet sedimentation adjustment	1.0	1.8
ice_sed_ai	Ice droplet fall speed parameter	500	1200
micro_mg_accre_enhan_fac	Liquid cloud accretion adjustment	1.5	1.75
micro_mg_berg_eff_factor	WBF process adjustment	0.1	0.7
prc_exp1	Exponent of liquid droplet number concentration in autoconversion	-1.2	-1.4
so4_sz_thresh_icenuc	Aitken model sulfate aerosol size threshold for homogeneous ice nucleation	0.05e-6	0.8e-6
wsubmin	Minimum subgrid vertical velocity used for liquid droplet nucleation	0.2	0.001

ZM Changes	Description	EAMv1	EAMv1P
alfa	Downdraft mass flux fraction adjustment	0.1	0.14
c0_lnd	Coefficient for convective cloud water to rain over land	0.007	0.002
c0_ocn	Coefficient for convective cloud water to rain over land	0.007	0.002
dmpdz	Parcel fractional mass entrainment rate	-0.7e-3	-1.2e-3
dp1	Deep convective cloud fraction parameter	0.045	0.018
ice_deep	Ice particle radius detrained from deep convection	16.e-6	14.e-6
mx_bot_lyr_adj	Adjustment for searching the maximum moist static energy	2	1

Aerosol changes	Description	EAMv1	EAMv1P
seasalt_emis_scale	Adjustment for sea spray aerosol mobilization	0.85	0.60
dust_emis_fact	Adjustment for dust mobilization	2.05	2.8

Estimated Inversion Strength

Wood and Bretherton (2006)

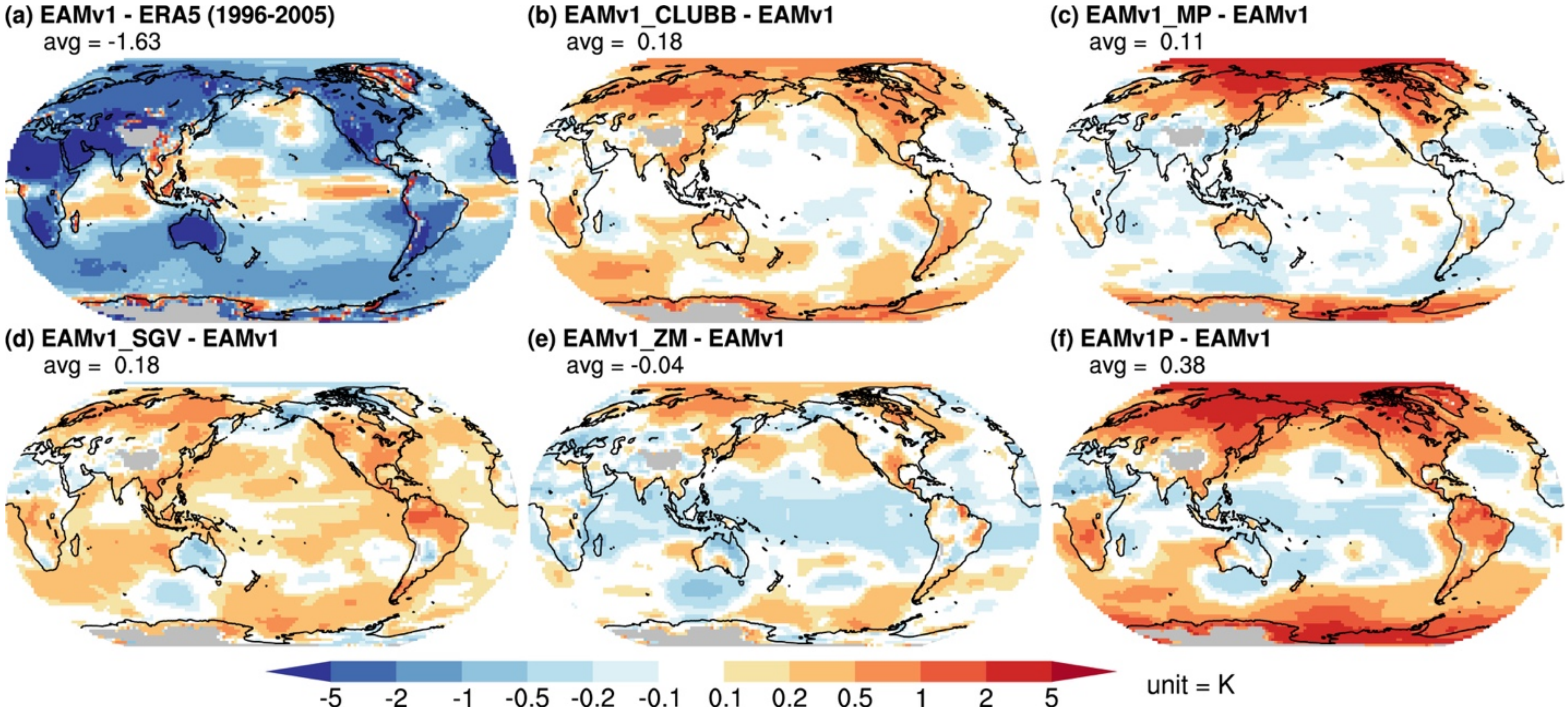

Frequency of decoupled PBL

Jones et al. (2011)

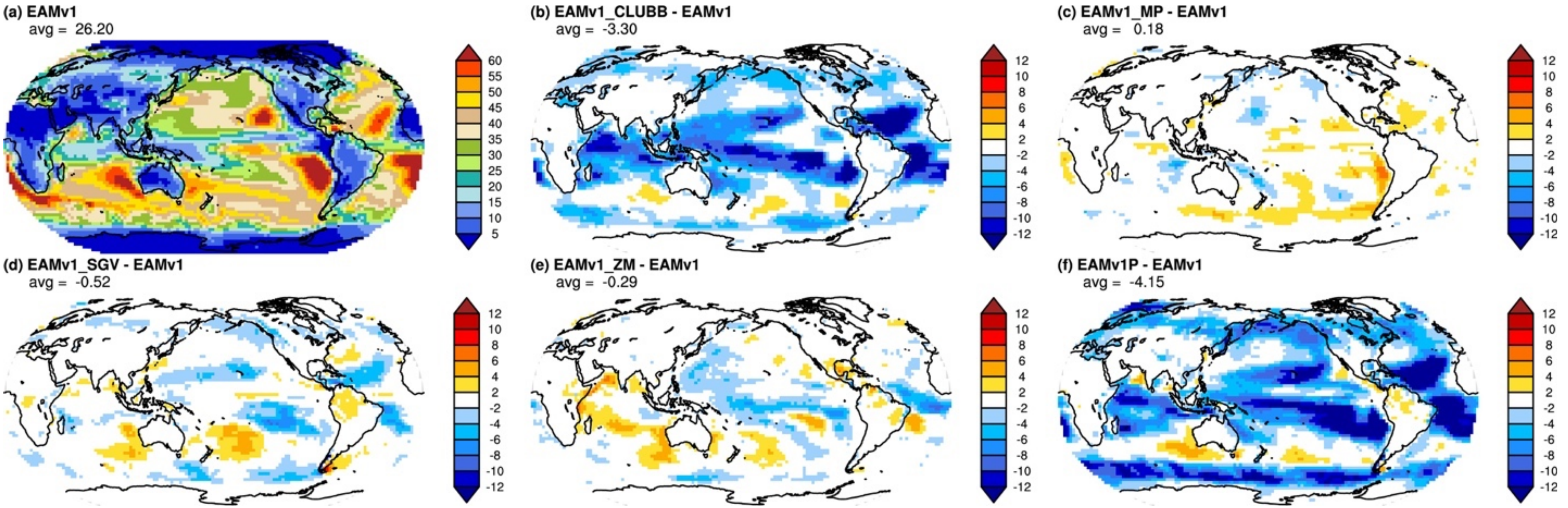

Cloud-top Entrainment Efficiency

Bretherton et al. (2007)

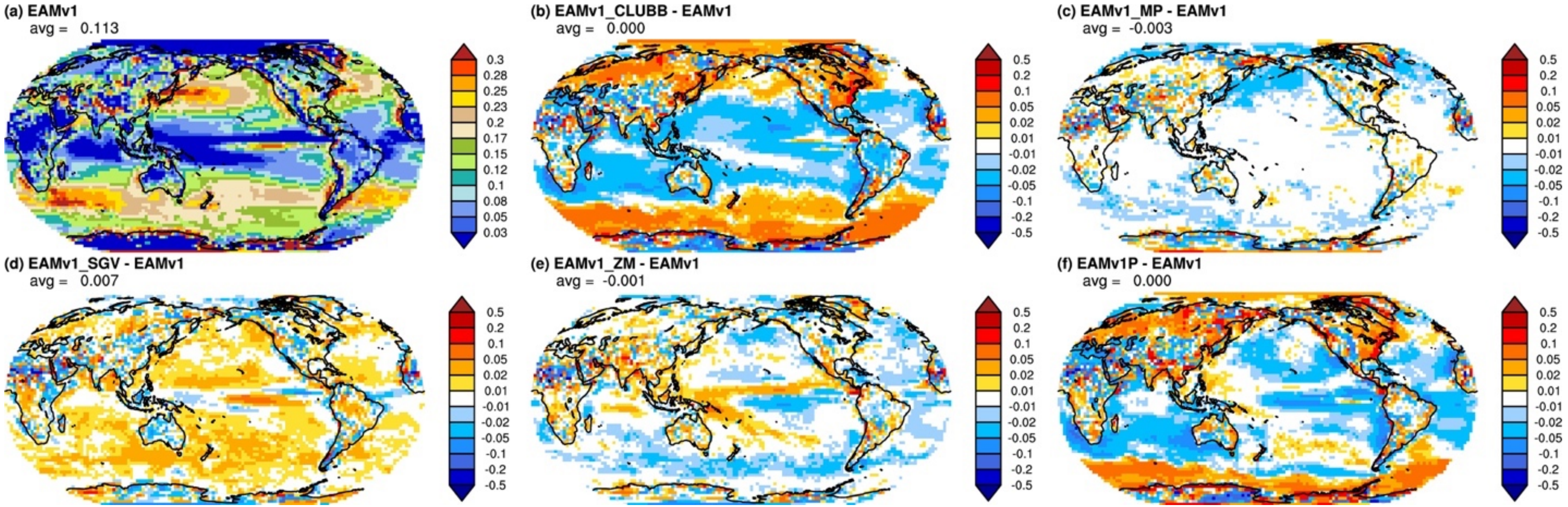

$A = w_e \Delta b\, z^i / w_*^3$

w_e: entrainment rate computed by differencing the resolved vertical motion and change of inversion height (Z_i)

Δb: virtual potential temperature jump scaled into buoyancy jump ($\Delta b = g\frac{\Delta\theta_v}{\theta_{ref}}$); θ_{ref} = 300 K

w_*: convective velocity ($w_* = (2.5 \int_0^{Z_i} \overline{w'b'} dz)^{1/3}$) that measures the buoyancy integrated over the boundary layer where b' is the buoyancy perturbation

Shortwave CRE shows significant improvements

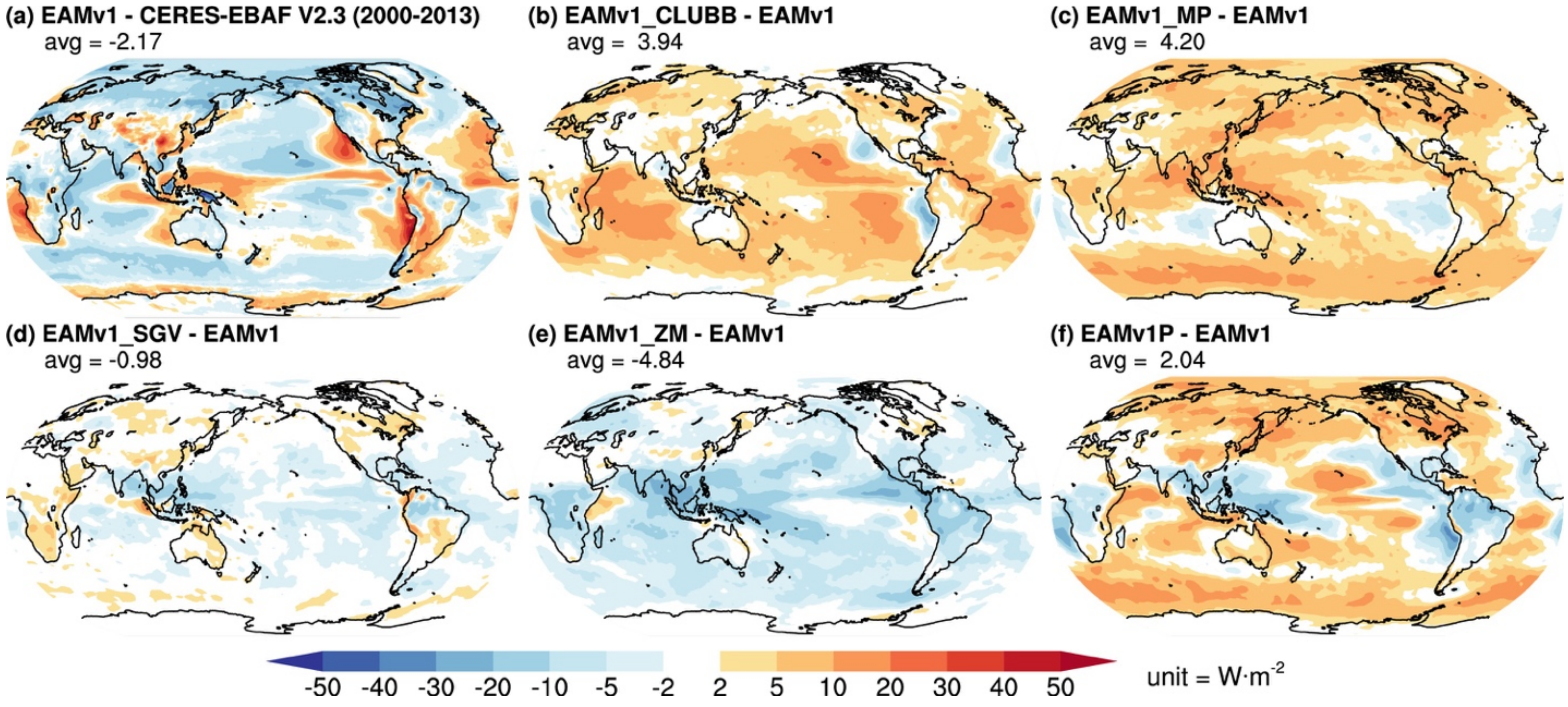

Precipitation improvements (associated with circulation improvements)

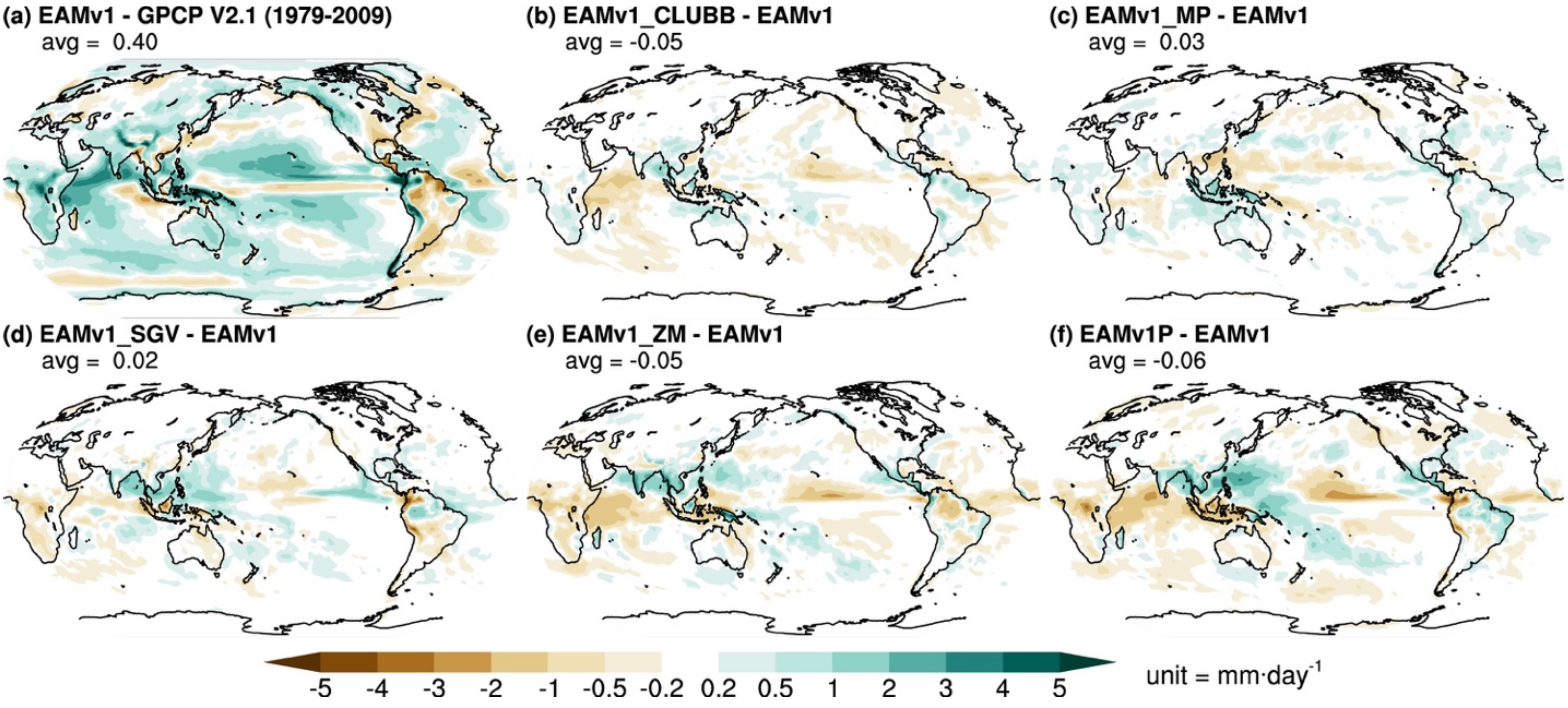

Surface temperature

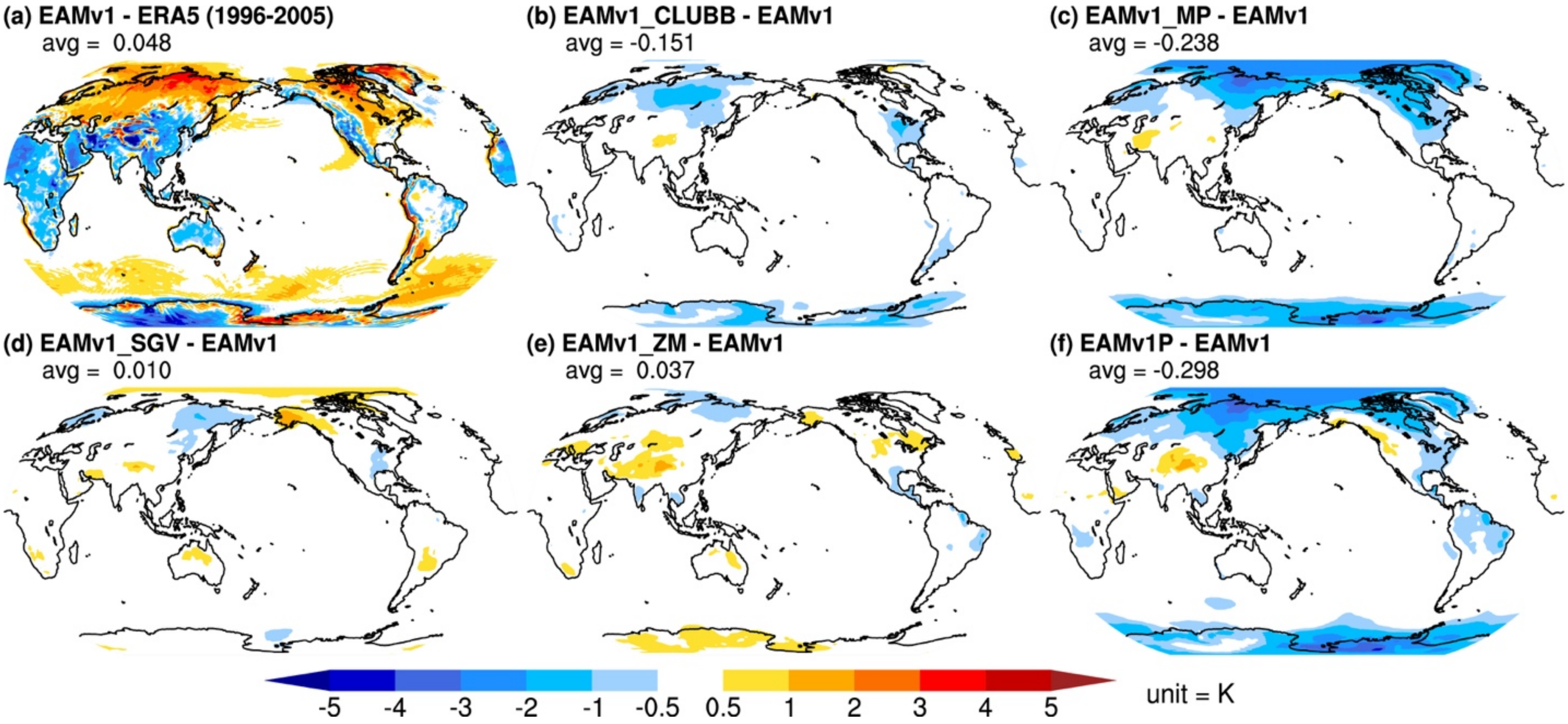

Surface wind

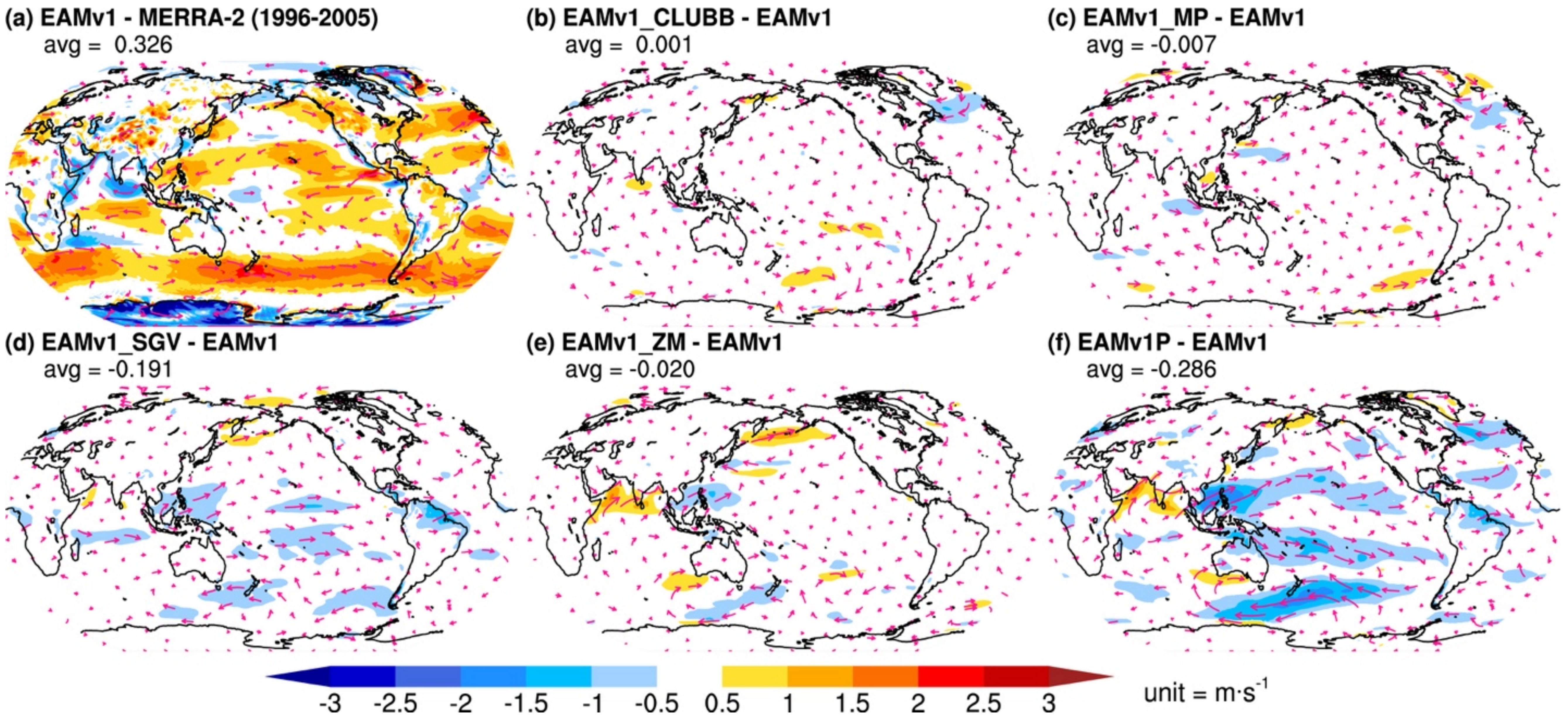

Precipitation timing

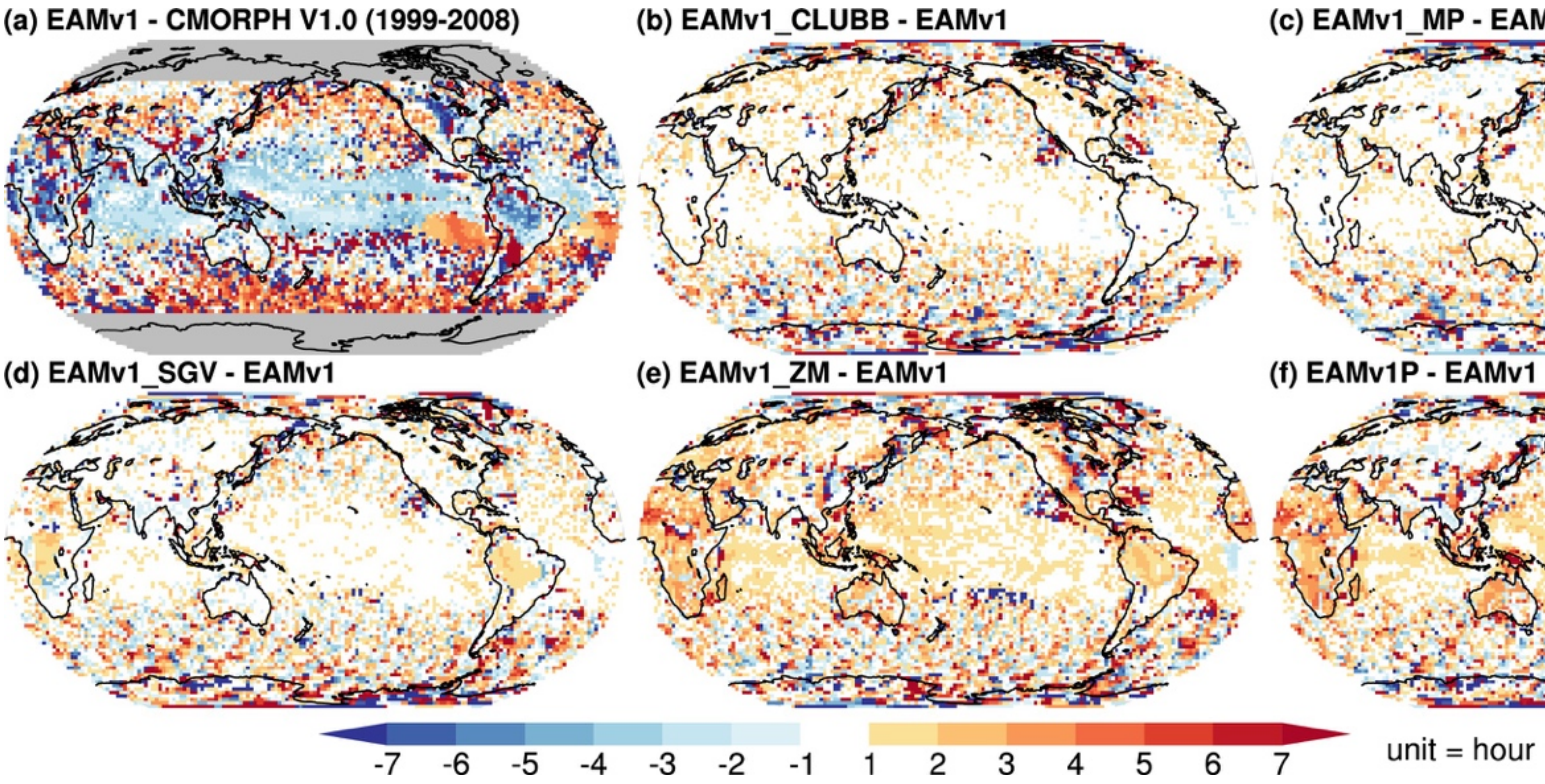

Role of aerosols in Earth's energy budget is a major source of uncertainty for earth system models and a significant issue for E3SMv1

IPCC AR5

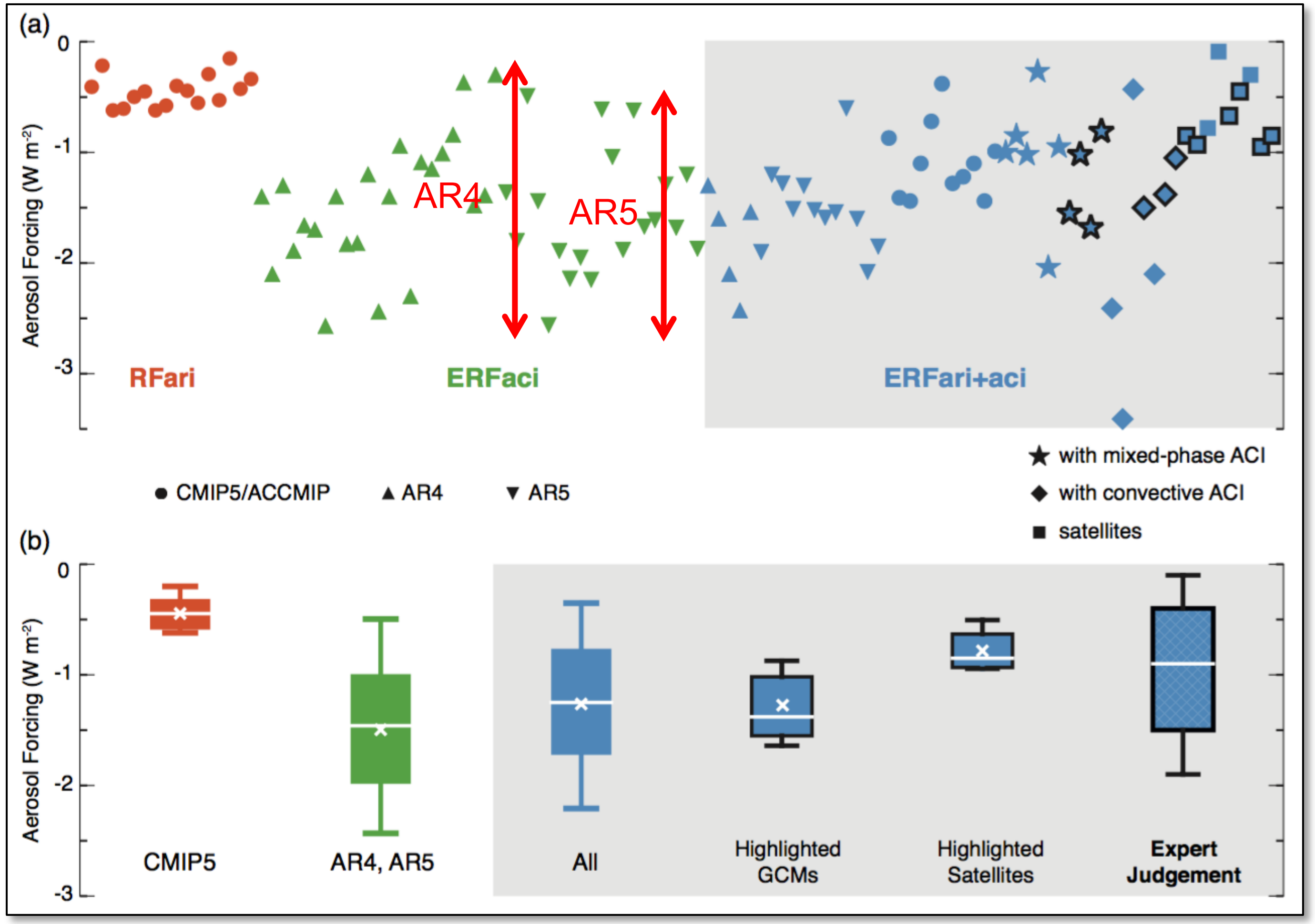

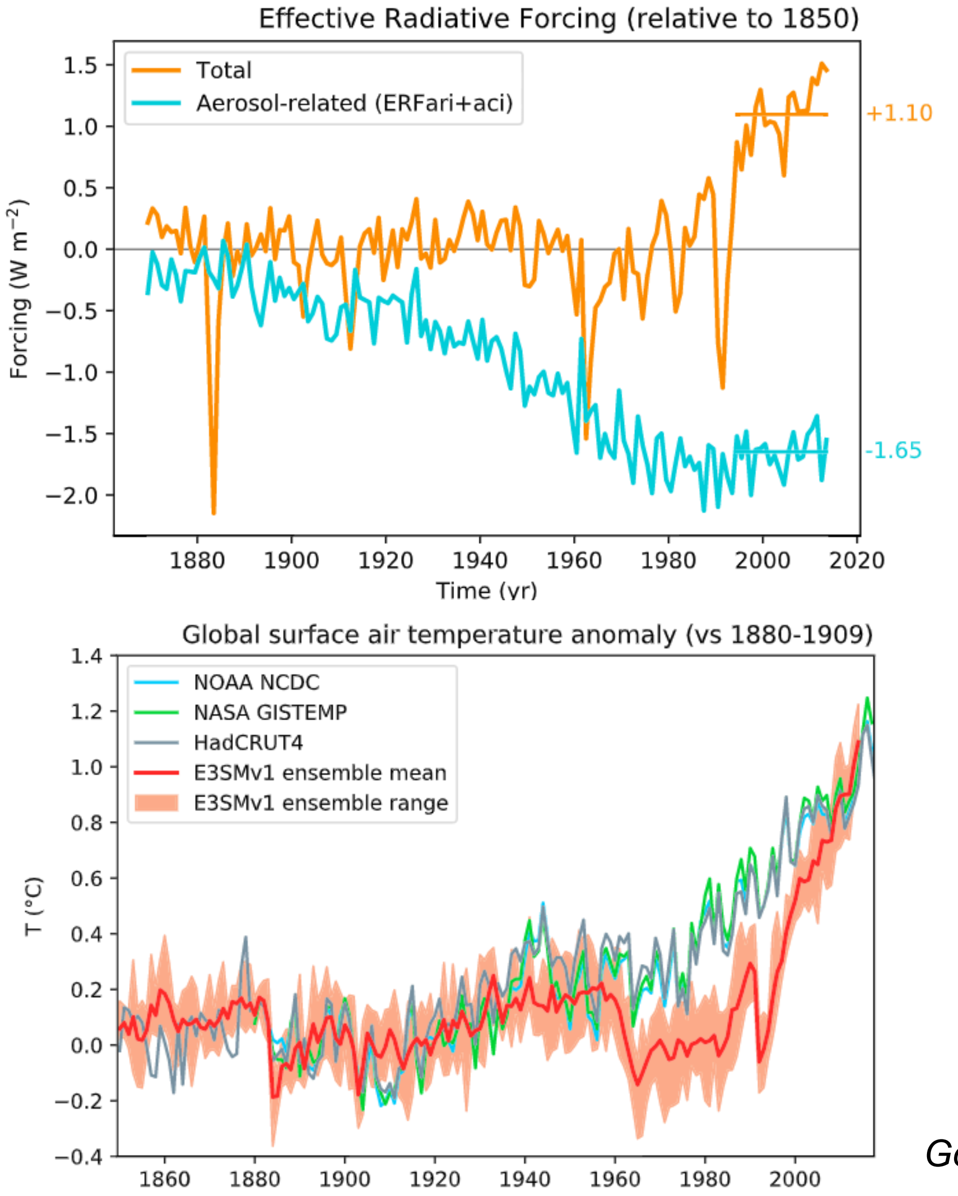

Golaz et al., 2019

Pacific Northwest NATIONAL LABORATORY

Convective Mixing (S+D)

Sherwood et al. (2014)

	EAMv1	EAMv1_CLUBB	EAMv1_MP	EAMv1_SGV	EAMv1_ZM	EAMv1P
S	0.40	0.40	0.41	0.41	0.38	0.38
D	0.21	0.21	0.20	0.20	0.19	0.17
LTMI (S+D)	0.61	0.61	0.61	0.61	0.57	0.55

Aerosol effects on CREs

	EAMv1	EAMv1_CLUBB	EAMv1_MP	EAMv1_SGV	EAMv1_ZM	EAMv1P
RFaci,sw	-1.53	-1.63	-0.95	-1.63	-1.62	-0.91
RFaci,lw	0.52	0.56	0.22	0.56	0.42	0.06
RFaci	-1.01	-1.07	-0.73	-1.07	-1.20	-0.85

Feedback decomposition

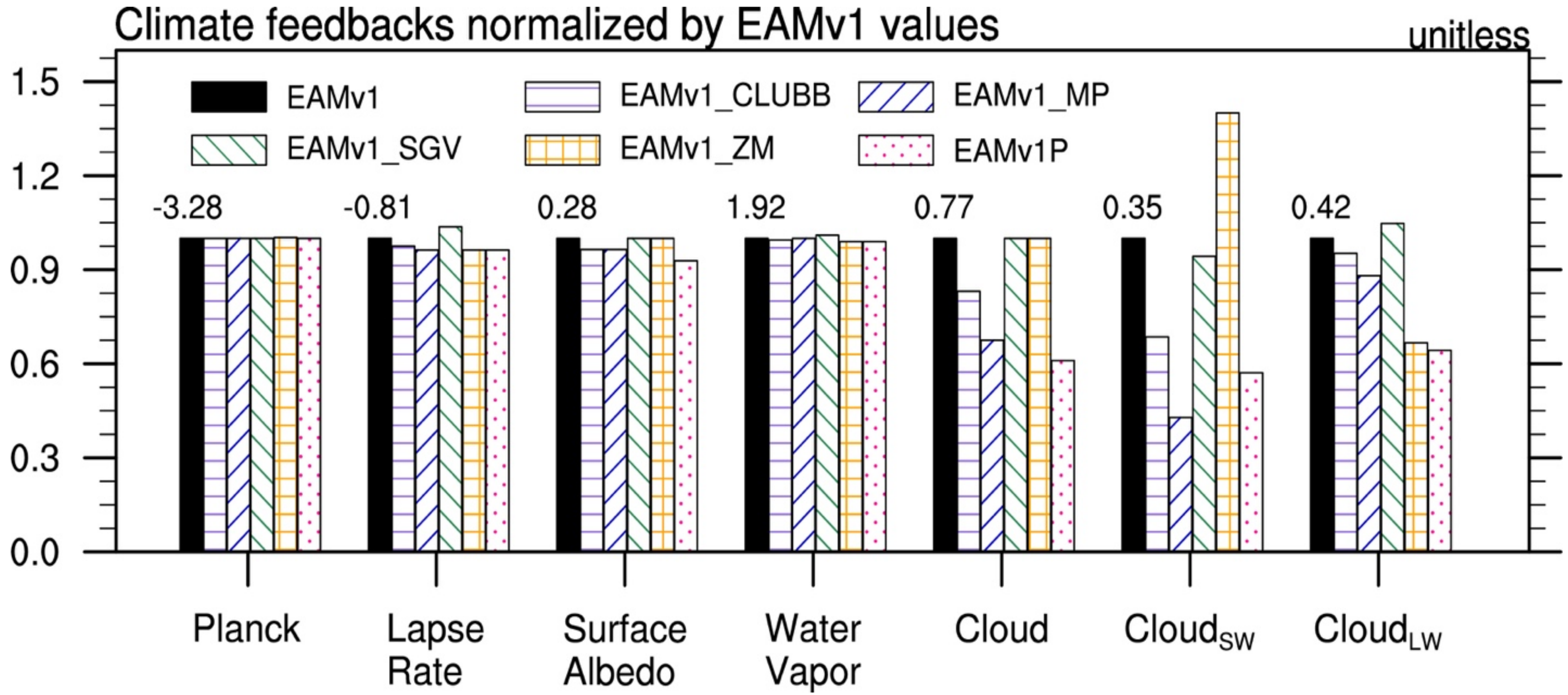

Summary

- This study develops a new model configuration with improved fidelity using a model calibration strategy that focuses on clouds.
- Governed by understanding of the physical mechanisms, the recalibration significantly improves the simulated clouds and precipitation, reducing common and longstanding biases across cloud regimes.
- With improved clouds, the atmosphere manifests itself to reduce biases in many aspects and shows minimal or no degradation in other aspects.
- Cloud and precipitation responses to aerosol and surface temperature perturbations are significantly weaker in the recalibrated model.
- This is a sensitivity study.